Change Point Detection in Knee Acoustic Emissions using the Teager Operator: A Preliminary Study in Patients with Juvenile Idiopathic Arthritis

Beren Semiz
Georgia Institute of Technology
Atlanta, GA, USA.
bsemiz@gatech.edu

Sinan Hersek
Georgia Institute of Technology
Atlanta, GA, USA.
shersek3@gatech.edu

Daniel C. Whittingslow
Emory School of Medicine
Atlanta, GA, USA.
d.c.whittingslow@emory.edu

Lori Ponder
Emory School of Medicine
Atlanta, GA, USA.
laponde@emory.edu

Sampath Prahalad
Emory School of Medicine
Atlanta, GA, USA.
sprahal@emory.edu

Omer T. Inan
Georgia Institute of Technology
Atlanta, GA, USA.
omer.inan@ece.gatech.edu

***Abstract*— Acoustic emission events (clicks) produced by the knee during movement have a variety of causes but can be classified as physiologic or pathologic. In this paper, we present a pilot study investigating detection and classification of physiologic and pathologic clicks in knee acoustic emissions from 4 subjects with juvenile idiopathic arthritis (JIA) and 4 control subjects. First, the signals are filtered and spectral noise suppression is applied. Then, the clicks are located using the Teager energy operator and are extracted from the main signals. Several time and frequency domain features are extracted from each click. Using a random forest classifier, the clicks are categorized as "physiologic" or "pathologic". In our dataset, we found an accuracy, sensitivity and precision of 94.3%, 93.3% and 96.6%, respectively, in correctly attributing these clicks to their respective classes. Similarly, the area under the receiver operating characteristics (ROC) curve is calculated as 0.98. The proposed click detection and classification pipeline may be used as an objective guide for knee health assessment in future work.**

Keywords—Wearable Technologies, knee joint health, acoustics.

I. INTRODUCTION

Juvenile idiopathic arthritis (JIA) is the most common rheumatic condition of childhood, affecting more than 200,000 children in the United States [1]. The origin and pathogenesis of JIA are still largely unknown. Joints affected with JIA undergo painful and progressive joint destruction. Early detection and appropriate treatment of JIA are crucial for preventing these long-term consequences. One of the most commonly affected joints in JIA is the knee joint [2, 3]; however, there is not a quantitative scheme for assessing the disease state in affected knees conveniently and accurately.

In previous work [4], we discussed the compelling need for an unobtrusive, quantitative and affordable joint-health assessment method. We leveraged the use of the sounds that joints make during movement to propose a biomarker of underlying joint health. These sounds can be measured on the surface of the skin and in the case of the knee likely originate from friction between articulating surfaces [5]. These signals are referred to as "vibroarthographic" signals in literature. Since Blodgett pioneered the use of these signals in 1902, many advances have been made in this field [6-8]. The development and application of piezoelectric accelerometers to joint sounds greatly advanced the field of vibroarthography [9, 10].

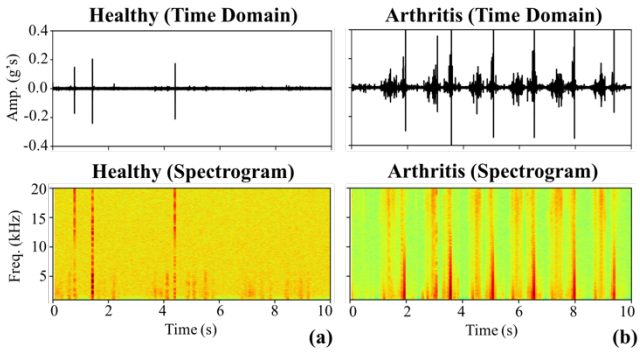

Fig.1: (a) Time domain signal and corresponding spectrogram of a recording taken from a control subject with physiological clicks. (b) Time domain signal and corresponding spectrogram of a recording taken from a subject with JIA

Previously, we developed a hardware setup and signal analysis algorithm to assess knee-joint health [4]. The proposed algorithm was validated with the measurements taken from 4 control subjects with no history of knee injury or pathology and 4 subjects diagnosed with JIA with affected knees. Several time and frequency domain features were extracted from the acoustic emission signals and fed into a soft classifier which is based on gradient boosting trees. Using leave-one-subject-out cross-validation (LOSO-CV), each subject was given a "knee audio score" ranging from 0 to 1, with 0 being a healthy knee and 1 being an involved joint. Although the cross-validated accuracy of the signal frames was high (92.3%), there remained an important observation and a potential drawback for the proposed algorithm. There were clicks that occurred in the

This material is based upon work supported in part by the Pediatric Technology Center (Georgia Tech and Children's Healthcare of Atlanta), the Marcus Foundation, Inc., Atlanta, GA, the National Institutes of Health, National Institute of Biomedical Imaging and Bioengineering, Grant No. 1R01EB023808, as part of the NSF/NIH Smart and Connected Health Program, and the National Science Foundation CAREER Award, Grant No. 1749677.

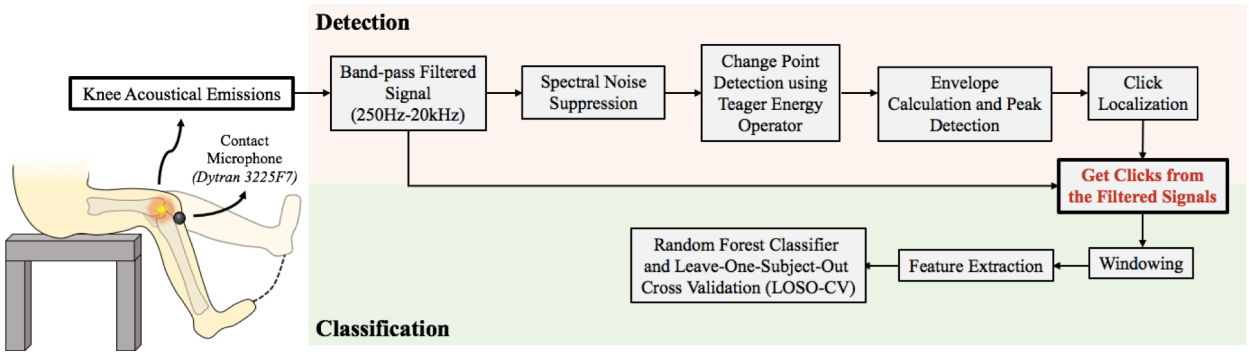

Fig.2: Detection and classification pipeline. Knee acoustic emissions are filtered, and spectral noise suppression is applied. Using the Teager energy operator, change points (in our case "clicks") are detected. Using these click locations, 100ms long click segments are extracted from the signals. Clicks are windowed, and time and frequency domain features are extracted from each window. Using the random forest classifier and LOSO-CV, the clicks are categorized as "physiologic" or "pathologic".

healthy controls' joint sounds (Fig. 1(a)) that appeared to resemble the clicks seen in the joint sounds of patients with JIA (Fig. 1(b)). The previously proposed algorithm did not focus on distinguishing the source of these clicks or classifying the clicks as physiologic versus pathologic. These physiologic clicks may arise from bursting of bubbles in the synovial fluid, ligament snapping, or physiologic synovium catching. [11]. Although these physiologic clicks are generally not associated with joint or synovium pathology, they still differ from the silent baseline knee recordings in terms of their time and frequency domain characteristics. Therefore, to prevent any false positives during the analysis of joint sound recordings, these physiologic clicks should be detected precisely and be distinguished from the pathologic clicks.

We hypothesize that these physiologic and pathologic clicks have different characteristics and could be differentiated with an automated system allowing for more precise classification of knee health status. This paper presents a novel algorithm to distinguish between these pathologic clicks and physiologic clicks. First, the desired clicks are located and extracted from the band-pass filtered signals using a detection pipeline (Fig.2). These clicks are then classified as "physiologic" or "pathologic" using a random forest classification algorithm.

II. Methods

A. Human Subject Protocol

This study was conducted under a protocol approved by the Georgia Institute of Technology and Emory University Institutional Review Boards. Knee acoustic emissions from 4 control subjects and 4 subjects with JIA were acquired as described in [4]. The recorded signals were analyzed using Matlab (MathWorks, Natick, MA) and Python (Python Software Foundation, Beaverton, OR). In this paper, the recordings from the control subjects are compared against the recordings taken from patients with JIA prior to starting treatment. Post-treatment data is not included as the true nature of the clicks (pathologic vs. physiologic) could not be certainly known at this point.

B. Pre-processing and Acoustic Noise Suppression

The signals are pre-processed using a digital finite impulse response (FIR) band-pass filter with a 250Hz-20kHz bandwidth to reduce interface noise. Sound artifacts at the beginning and end of the recordings are removed manually (Fig.3(a)). After this preprocessing step, the spectral noise suppression algorithm developed by Ephraim and Malah [12] is employed to reduce the background noise. Each recording is segmented with Hanning windows and the corresponding short time Fourier transform (STFT) is computed to calculate the signal spectral power. Assuming that the noise is stationary, the power spectrum of the noise is computed using the small silent portions of the recordings where no clicks are present. For each frame, *a posteriori* (ratio of the noisy speech spectrum and the noise spectrum) and *a priori* (ratio of the clean speech spectrum and the noise spectrum) signal-to-noise ratio (SNR) values are calculated using the decision-directed approach described in [12]. The signal gain is updated after each frame and this gain vector is used to clean the actual STFT. Finally, the noise-reduced signal is reconstructed using inverse STFT and overlap-add methods (Fig.3(b)).

C. Teager Energy Operator

The Teager energy operator is a non-linear operator derived from the energy of a simple oscillator using the physics of motion. It represents the running estimate of the signal energy by operating on three sequential samples of the signal at a given time point [13]. In the discrete-time case, it is defined as:

$$\Psi_{TE}[n]=\boldsymbol{x}[n]^2 - \boldsymbol{x}[n+1]\boldsymbol{x}[n-1] \quad (1)$$

This operator is generally used to detect instantaneous changes in signals such as discontinuities, changes in signal amplitude and/or changes in frequency. Additionally, it suppresses the background activity and discards soft changes [14]. Knee acoustic emissions usually have high energy and short duration [4, 8], therefore, the Teager operator appears to be well-suited for detecting the instantaneous changes in these signals: specifically, the "clicks" in the recordings.

D. Click Detection

After computing the Teager energy operator, the locations of these change points are stored for each recording using a simple peak detection algorithm. First, the envelope of the Teager operator is generated, then the peaks which are greater than 20% of the range of the signal value are selected as the

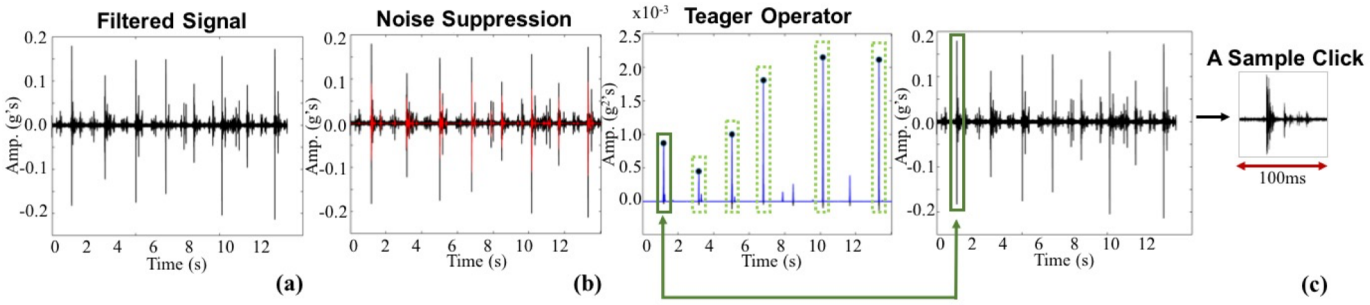

Fig.3: (a) The signals are filtered using a 250Hz-20kHz band-pass filter. (b) Spectral noise suppression is applied for background noise. (c) Using the Teager energy operator, change point locations are detected. Using this information, 100ms long click segments are clipped from the band-pass filtered signals.

potential click locations. This threshold is selected heuristically to include as many clicks as possible while ignoring small fluctuations in the signal. Using these clicks locations, the portions within *click location* ± 50ms are extracted from the main signals for each detected click. This 100ms window-length is selected to include the main click and its smaller, subsequent clicks (Fig.3(c)). A total of 53 clicks (30 from the involved knee recordings and 23 from the control recordings) are stored in matrix **Y** for further processing and classification.

E. Feature Extraction

Each 100ms-long click in matrix **Y** is segmented into 10ms windows using 50% overlap to increase the number of instances for the classification algorithm. This resulted in 954 frames in total (18 frames from each click), and time and frequency domain features are extracted from each frame. The wide bandwidth (250Hz to 20kHz) of the joint sounds causes these signals to have distinctive spectral features, whereas the spike-like appearances in the time domain result in unique time domain features. Thus, 8 total features are extracted: 3 in the time domain and 5 in the frequency domain. In the time domain, the zero crossing rate, energy, and energy entropy are calculated. In the spectral domain, the spectral flux, spectral spread, spectral entropy, spectral roll-off, and spectral centroid are calculated. The performance of these features and the importance of having a diverse feature set in knee acoustic emission analysis were previously discussed in [4]. These features are stored under the 954x8 matrix **X**.

F. t-Distributed Stochastic Neighbor Embedding (t-SNE)

To visualize the ability of our feature set to distinguish between the physiologic and pathologic clicks, dimensionality reduction using t-distributed stochastic neighbor embedding (t-SNE) is applied. This dimensionality reduction approach attempts to maintain the distances between points, which are defined based on their probabilities of being neighboring points, during mapping from high dimensional space to low dimensional space. Let x_i be a point in high dimensional space; so the conditional probability that x_i chooses x_j as its neighbor is $p_{i|j.}$ Similary, this probabilty can be defined as $q_{i|j}$ in low dimensional space. So t-SNE tries to minimize the mismatch between $p_{i|j}$ and $q_{i|j}$, and tries to find the best low-dimensional representation for the current data. [15].

In the current problem, each feature represents one dimension. Using t-SNE, the 8 dimensional data (with each dimension corresponding to one of the 8 features) is mapped onto 2 dimesional space for better visualization. After dimensionality reduction, a scatter plot with two axes, where each point is respresenting a 10ms signal frame, is constructed. Two colors are used to categorically label the data points - pathologic clicks in red and physiologic clicks in green.

G. Random Forest Classification

As previously explained, the clicks clipped from the filtered signals are windowed and 8 features are extracted from each frame. These features are stored in matrix **X**. The pathologic signals and physiologic signals are given the labels 1 and 0, respectively, and these labels are stored in 53x1 vector **w**. Random forest classification with 100 estimators and maximum depth value of 7 is employed to classify 954 frames from 53 physiologic or pathologic clicks. We chose random forest classifier, since it can achieve high accuracy values without causing any overfitting. Random forests are sets of trees with the same distribution where each tree depends on the values of an independently sampled random vector [16]. After several trees are generated, each tree casts a unit vote for the most popular class in the input data – in our case for "physiologic" and "pathologic" classes.

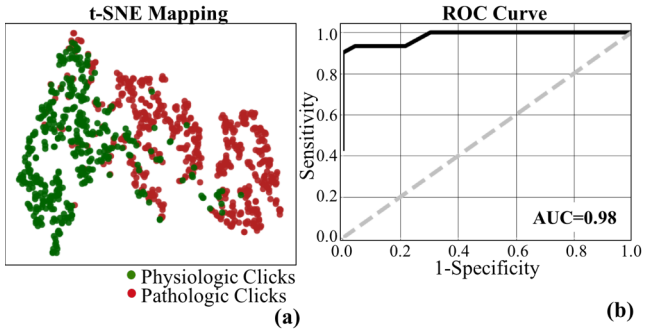

Fig.4: (a) t-SNE graph for the physiologic and pathologic clicks. (b) The ROC curve for the proposed model. The AUC is calculated to be 0.98.

The performance assessment is performed using leave-one subject-out cross validation (LOSO-CV). In each fold, all click frames from one subject are left out, and the model is trained on the remaining click frames from 7 subjects. Then the model is tested on the click frames of the subject being left out. This

procedure is completed for all 8 subjects and the predicted classes of the frames are stored in 53x18 matrix **Z**, where 53 is the number of clicks and 18 is the number of frames belonging to each click. These frame scores are then averaged to get the final score of each click and stored in 53x1 vector **h**. The clicks are classified as "pathologic" if the calculated score is greater than 0.5, an as "physiologic" if less than 0.5. Finally using the predicted scores in vector **h** and the actual classes in vector **w**, the performance metrics (accuracy, sensitivity and precision) are calculated and the corresponding receiver operating characteristics (ROC) curve is plotted.

III. Results and Discussion

A. t-Distributed Stochastic Neighbor Embedding (t-SNE)

The data from 4 subjects with JIA and 4 control subjects is visualized as described in Section II-F. In Fig.4(a) the corresponding t-SNE graph for the physiologic (green dots) and pathologic (red dots) clicks is presented. The frames from these two click types construct separate clusters in two dimensional space based on their time and spectral domain features. This seperation supports the ability of our feature set to distinguish between these two groups, and supports our hypothesis about these physiologic and pathologic clicks having different characteristics. Physiologic clicks may be caused by cavitation in the synovial fluid, ligaments snapping, etc. [11]. The causes of clicks in JIA are yet unknown, but are most likely attributed to the chronic inflammatory state of the synovium and cartilage degradation [17-19]. Since these clicks have different origins, it is reasonable that there would be differences in their time and frequency information.

B. Random Forest Classification

As explained in Section II-G, 53 physiologic and pathologic click frames are classified using random forest classifier and the model is validated using LOSO-CV. This led to cross validated accuracy, sensitivity and precision of 94.3%, 93.3% and 96.6%, respectively. Similarly, the ROC curve is plotted (Fig.4(b)), and the corresponding area under curve (AUC) is calculated to be 0.98. In biomedical applications, along with high accuracy, a high sensitivity value is preferred in the design of a screening test/technology, since this metric corresponds to the "detection rate" of the algorithm. In this study, we obtained a detection rate of 93.3%, which shows that this approach can detect and interpret the changes in joint sound signals. Thus, this algorithm could potentially be used to track and evaluate the knee health status of both healthy and diseased knees. In the future, this click-scoring pipeline could be extended beyond JIA to assist in rehabilitation and recovery following musculoskeletal injuries. Additionally, this signal differentiating capability could be utilized in remote monitoring or telemedicine frameworks. By using miniature sensors embedded in a wearable system, the joints could be continuously monitored and joint status changes or disease exacerbations could be detected or maybe even predicted. This early detection would improve patients' quality of life and reduce surgeries and healthcare costs.

IV. Conclusion

In this paper, we presented a new algorithm for detecting and classifying physiologic and pathologic clicks from the knees of subjects with JIA and healthy control subjects. An automated algorithm such as the one presented in this paper can potentially be used to assist clinical decision making and provide knee-health tracking in wearable systems for home-monitoring. In future studies, we will validate our findings with larger datasets and attempt not only supervised learning algorithms, but also unsupervised ones to ensure the generalizability of our approach.

References

[1] C. G. Helmick, D. T. Felson, R. C. Lawrence, S. Gabriel, R. Hirsch, C. K. Kwoh*, et al.*, "Estimates of the prevalence of arthritis and other rheumatic conditions in the United States: Part I," *Arthritis & Rheumatism,* vol. 58, pp. 15-25, 2008.

[2] J. C. Packham and M. A. Hall, "Long-term follow-up of 246 adults with juvenile idiopathic arthritis: functional outcome," *Rheumatology (Oxford),* vol. 41, pp. 1428-35, Dec 2002.

[3] A. D. Woolf and B. Pfleger, "Burden of major musculoskeletal conditions," *Bull World Health Organ,* vol. 81, pp. 646-56, 2003.

[4] B. Semiz, S. Hersek, D. C. Whittingslow, L. A. Ponder, S. Prahalad, and O. T. Inan, "Using Knee Acoustical Emissions for Sensing Joint Health in Patients With Juvenile Idiopathic Arthritis: A Pilot Study," *IEEE Sensors Journal,* vol. 18, pp. 9128-9136, 2018.

[5] Y. Wu, *Knee joint vibroarthrographic signal processing and analysis*: Springer, 2015.

[6] W. E. Blodgett, "Auscultation of the knee joint," *The Boston Medical and Surgical Journal,* vol. 146, pp. 63-66, 1902.

[7] A. Steindler, "Auscultation of joints," *JBJS,* vol. 19, pp. 121-136, 1937.

[8] M. L. Chu, I. A. Gradisar, M. R. Railey, and G. F. Bowling, "An electro-acoustical technique for the detection of knee joint noise," *Med Res Eng,* vol. 12, pp. 18-20, 1976.

[9] R. A. B. Mollan, "Vibration emission in bone and joints," Ph.D. Dissertation, Queen's University, 1981.

[10] D. A. Winter, *Biomechanics and motor control of human movement*: John Wiley & Sons, 2009.

[11] S. J. Song, C. H. Park, H. Liang, and S. J. Kim, "Noise around the Knee," *Clin Orthop Surg,* vol. 10, pp. 1-8, Mar 2018.

[12] Y. Ephraim and D. Malah, "Speech enhancement using a minimum-mean square error short-time spectral amplitude estimator," *IEEE Transactions on acoustics, speech, and signal processing,* vol. 32, pp. 1109-1121, 1984.

[13] J. F. Kaiser, "On a simple algorithm to calculate the'energy'of a signal," in *Acoustics, Speech, and Signal Processing, 1990. ICASSP-90., 1990 International Conference on*, 1990, pp. 381-384.

[14] A. Erdamar, F. Duman, and S. Yetkin, "A wavelet and teager energy operator based method for automatic detection of K-Complex in sleep EEG," *Expert Systems with Applications,* vol. 39, pp. 1284-1290, 2012.

[15] L. v. d. Maaten and G. Hinton, "Visualizing data using t-SNE," *Journal of machine learning research,* vol. 9, pp. 2579-2605, 2008.

[16] L. Breiman, "Random forests," *Machine learning,* vol. 45, pp. 5-32, 2001.

[17] S. Nalband, A. Sundar, A. A. Prince, and A. Agarwal, "Feature selection and classification methodology for the detection of knee-joint disorders," *Computer methods and programs in biomedicine,* vol. 127, pp. 94-104, 2016.

[18] I. Nakamura, K. Michishita, M. Tanno, and K. Ito, "Synovial impingement after posterior cruciate-retaining total knee arthroplasty for rheumatoid arthritis," *Journal of Orthopaedic Science,* vol. 11, pp. 303-307, 2006.

[19] A. Ravelli, "Toward an understanding of the long-term outcome of juvenile idiopathic arthritis," *Clinical and experimental rheumatology,* vol. 22, pp. 271-275, 2004.